Published in final edited form as:
J Biol Chem. 2004 March 5; 279(10): 9557–9564. doi:10.1074/jbc.M310512200.

ATP-Citrate Lyase Deficiency in the Mouse*

Anne P. Beigneux[‡,§,¶], **Cynthia Kosinski**[‡], **Bryant Gavino**[‡], **Jay D. Horton**[‖,**], **William C. Skarnes**[§§], and **Stephen G. Young**[‡,§,‡‡]

[‡]Gladstone Institute of Cardiovascular Disease, University of California, San Francisco, California 94141-9100

[§]Cardiovascular Research Institute, University of California, San Francisco, California 94141-9100

[‖]Department of Molecular Genetics, University of Texas Southwestern Medical Center, Dallas, Texas 75390-9046

[**]Department of Internal Medicine, University of Texas Southwestern Medical Center, Dallas, Texas 75390-9046

[‡‡]Department of Medicine, University of California, San Francisco, California 94141-9100

[§§]Department of Molecular and Cell Biology, University of California, Berkeley, California 94720

Abstract

ATP-citrate lyase (Acly) is one of two cytosolic enzymes that synthesize acetyl-coenzyme A (CoA). Because acetyl-CoA is an essential building block for cholesterol and triglycerides, Acly has been considered a therapeutic target for hyperlipidemias and obesity. To define the phenotype of *Acly*-deficient mice, we created *Acly* knockout mice in which a β-galactosidase marker is expressed from *Acly* regulatory sequences. We also sought to define the cell type-specific expression patterns of *Acly* to further elucidate the *in vivo* roles of the enzyme. Homozygous *Acly* knockout mice died early in development. Heterozygous mice were healthy, fertile, and normolipidemic on both chow and high fat diets, despite expressing half-normal amounts of *Acly* mRNA and protein. Fibroblasts and hepatocytes from heterozygous *Acly* mice contained half-normal amounts of *Acly* mRNA and protein, but this did not perturb triglyceride and cholesterol synthesis or the expression of lipid biosynthetic genes regulated by sterol regulatory element-binding proteins. The expression of acetyl-CoA synthetase 1, another cytosolic enzyme for producing acetyl-CoA, was not up-regulated. As judged by β-galactosidase staining, *Acly* was expressed ubiquitously but was expressed particularly highly in tissues with high levels of lipogenesis, such as in the livers of mice fed a high-carbohydrate diet. β-Galactosidase staining was intense in the developing brain, in keeping with the high levels of *de novo* lipogenesis of the tissue. In the adult brain, β-galactosidase staining was in general much lower, consistent with reduced levels of lipogenesis; however, β-galactosidase expression remained very high in cholinergic neurons, likely reflecting the importance of Acly in generating acetyl-CoA for acetylcholine synthesis. The *Acly* knockout allele is useful for identifying cell types with a high demand for acetyl-CoA synthesis.

ATP-citrate lyase (Acly)[1] is a cytosolic enzyme that catalyzes the formation of acetyl-coenzyme A (CoA) and oxaloacetate from citrate and CoA, with the hydrolysis of ATP to ADP

*This work was supported by National Institutes of Health NHLBI Program in Genomics Applications Grants "BayGenomics" HL66621, HL66600, and HL66590.

[¶]To whom correspondence should be addressed: Gladstone Institute of Cardiovascular Disease, P. O. Box 419100, San Francisco, CA 94141-9100. Tel.: 415-826-7500; Fax: 415-285-5632; abeigneux@gladstone.ucsf.edu.

and phosphate. Acetyl-CoA is the key building block for *de novo* lipogenesis. Acly is not, however, the sole source of acetyl-CoA in the cytosol. Another enzyme, acetyl-CoA synthetase 1 (Acs1), generates acetyl-CoA from acetate and CoA, with the hydrolysis of ATP to AMP and diphosphate (1). Whether Asc1 might be sufficient in the setting of a genetic deficiency in Acly is not known. The expression of both Acly and Acs1 is controlled by the sterol regulatory element-binding protein (SREBP)-1c, a transcriptional regulator of fatty acid synthesis (2,3).

An important role for Acly in lipid biosynthesis in the liver has been suggested by studies with the Acly inhibitor hydroxycitrate. In rats treated with hydroxycitrate, the rate of fatty acid and cholesterol synthesis in the liver fall (4). Those experiments and studies with other inhibitors (5–10) have suggested that Acly could represent a therapeutic target for elevated plasma lipid levels. As with other genes involved in lipid synthesis, the expression of *Acly* in the liver is regulated, at least in part, at the transcriptional level by SREBP-1 (3,11,12). When lipid biosynthesis levels in the liver are low, as in fasted mice, *Acly* mRNA levels are low. However, when fasted mice are fed a carbohydrate-rich diet, lipid biosynthesis rates and *Acly* mRNA levels increase (3,12).

Lipid synthesis is important in the developing brain, particularly for myelination (13). Northern blots have shown that *Acly* mRNA levels increase in the rat brain during the first week of suckling, when *de novo* lipogenesis is high (14). However, those experiments have not revealed which regions of the brain, or which cell types in the brain, express *Acly* at high levels. Acly is also highly expressed in the kidney (15,16), and moderate amounts of the *Acly* mRNA are found in the adrenals, intestine, and lung (14).

In this study, we explored the physiologic importance of *Acly* in mice. We had three goals. First, we were interested in determining if a complete absence of Acly would be compatible with embryonic development. Second, we wanted to determine whether half-normal levels of Acly, as in heterozygous *Acly* knockout mice, would be associated with alterations in lipid synthesis, plasma lipid levels, or body weight. Third, we sought to define the cell type-specific expression of *Acly*, both during development and in adult mice, to better understand the *in vivo* roles of Acly. To address these questions, we produced and characterized *Acly*-deficient mice.

EXPERIMENTAL PROCEDURES

Acly-deficient Mice

A mouse embryonic stem cell line (cell line NPX098, strain 129/Ola) containing an insertional mutation in *Acly* was identified within BayGenomics, a gene-trapping resource (17). The gene-trap vector used (pGT1δTMpfs) contains a splice-acceptor sequence upstream of a reporter gene, β*geo* (a fusion of β-galactosidase and neomycin phosphotransferase II) (17). As judged by 5′ rapid amplification of cDNA ends (18), the insertional mutation in NPX098 occurred in the first intron of *Acly*, following a noncoding first exon. Thus, the mutation results in the production of a fusion transcript consisting of exon 1 sequences from *Acly* and β*geo*. The mutation created a new EcoRV site in intron 1, which was useful for genotyping mice by Southern blots (see below).

NPX098 was injected into C57BL/6 blastocysts to generate chimeric mice, which were bred to establish *Acly* knockout mice. All mice described herein had a mixed genetic background

[1]The abbreviations used are: Acly, ATP-citrate lyase; Acs1, acetyl-CoA synthetase 1; SREBP, sterol regulatory element-binding protein; βgeo, a fusion of β-galactosidase and neomycin phosphotransferase II; Gapdh, glyceraldehyde-3-phosphate dehydrogenase; dpc, days post-coitus.

(~50% C57BL/6 and ~50% 129/Ola). The mice were weaned at 21 days of age, housed in a barrier facility with a 12-h light/12-h dark cycle, and fed a chow diet containing 4.5% fat (Ralston Purina, St. Louis, MO). In some experiments, the mice were fed a Western diet (21% fat, 50% carbohydrate, and 20% protein) from Research Diets (New Brunswick, NJ) or a fat-free, carbohydrate-rich diet (60.2% sucrose and 20% casein) from ICN (Irvine, CA).

Mice were genotyped by Southern blots with EcoRV-digested genomic DNA and a 5′ *Acly* flanking probe. The probe was amplified from mouse genomic DNA with primers 5′-CGCTGGTCAAGAATGGGTGTTACAA-3′ and 5′-CTCCCTCCCCCAACCTCAAACTAAG-3′.

Mouse Primary Embryonic Fibroblasts

Timed matings were established between *Acly*+/− mice, and pregnant females were sacrificed 13.5–17.5 days post-coitus (dpc). Embryos were incubated overnight in 5 ml of 0.25% trypsin-EDTA (Invitrogen, Carslbad, CA) at 4 °C. The next morning, embryos were mechanically disrupted in 5 ml of Dulbecco's modified Eagle's medium supplemented with fetal bovine serum, L-glutamine, nonessential amino acids, penicillin, streptomycin, Fungizone (Invitrogen), and 2-mercaptoethanol (Sigma). After removal of debris, cells were plated in 100-mm Petri dishes.

Mouse Primary Hepatocytes

Mice were anesthetized with 2.5% avertin, and a catheter was introduced into the inferior vena cava via the right atrium. The liver was perfused with liver perfusion media (Invitrogen) and then collagenase-lipase media (Invitrogen). The digested liver was then removed and mechanically disrupted. The cell suspension was filtered through sterile gauze and centrifuged at 50 × *g*. Hepatocytes were then washed three times with hepatocyte wash media (Invitrogen), and 5×10^5 cells/well were plated in 6-well collagen-coated tissue culture plates. Cells were allowed to attach to the plate for 4 h before starting the labeling experiments (see below). Cells were grown at 37 °C under 5% CO_2 in 3 ml of Dulbecco's modified Eagle's medium supplemented with fetal bovine serum, sodium pyruvate, L-glutamine, nonessential amino acids, penicillin, streptomycin, and Fungizone.

Analysis of Cholesterol and Triglyceride Synthesis by Thin-layer Chromatography

Acly+/+ and *Acly*+/− fibroblasts were grown to 90% confluency in 100-mm Petri dishes. Cells were then labeled with 50 μCi of [1(3)-^{3}H]glycerol (Amersham Biosciences), 10 μCi of [1,5-^{14}C]citric acid (American Radiolabeled Chemicals, St. Louis, MO), or 25 μCi of [1-^{14}C] acetic acid (Amersham Biosciences). Primary hepatocytes were labeled with 10 μCi of [1 (3)-^{3}H]glycerol. Lipids from fibroblasts and hepatocytes were extracted with hexane:isopropyl alcohol (3:2 (v/v)), dried under nitrogen, and resuspended in 100 μl of chloroform. Triglycerides and free cholesterol were separated on thin-layer chromatography silica plates (60 Å) in hexane:ethyl ether:acetic acid (80:20:1 (v/v/v)). Samples were assayed in duplicates (40 μl/lane). After lipid extraction, cell protein was quantified with the Bradford assay (Bio-Rad).

Blood samples were taken from the retroorbital sinus under anesthesia (2.5% avertin). Plasma cholesterol, triglycerides, and free fatty acids were measured with enzymatic assays (Abbott Spectrum (Abbott, Abbott Park, IL), triglycerides/glycerol blanked (Roche/Hitachi, Indianapolis, IN), and free fatty acids half-micro test (Roche Applied Science), respectively). Liver lipids were extracted (19), and the amounts of cholesterol and triglycerides were measured (20). Before harvesting of liver tissue, mice were anesthetized and perfused with saline.

RNA Isolation and Northern Blot Analysis

Total RNA was isolated from 50 to 150 mg of mouse tissue or from fibroblasts grown on 100-mm Petri dishes with Tri-Reagent (Sigma). Total RNA (25 μg) was separated by electrophoresis on a 1% agarose/formaldehyde gel and transferred onto a Nytran SuPerCharge membrane (Schleicher & Schuell). A mouse multiple-tissue poly(A)$^+$ RNA blot and a mouse embryo poly(A)$^+$ RNA blot (Clontech, Palo Alto, CA) were used to determine the tissue pattern of *Acly* expression in adult mice and to examine the temporal expression of *Acly* during embryogenesis. Bands on Northern blots were visualized by autoradiography (Hyperfilm ECL, Amersham Biosciences) and quantified by densitometry (Molecular Imager FX, Bio-Rad). We used the same *Acly* cDNA probe that has been described previously (11). A β-galactosidase cDNA was amplified by reverse transcriptase-PCR from *Acly*+/− mouse liver RNA with primers 5′-TTTTCGATGAGCGTGGTGGTTATGC-3′ and 5′-GCGCGTACATCGGGCAAATAATATC-3′; an *Asc1* cDNA was amplified with oligonucleotides 5′-TGCTGAGGACCCACTCTTCATCTTG-3′ and 5′-AAGCAGAACCAGGTTTCATGGGTGT-3′. A glyceraldehyde-3-phosphate dehydrogenase (*Gapdh*) probe and an 18 S cDNA were used as controls for RNA integrity and loading. [α-^{32}P]dCTP-labeled cDNA probes were prepared with All-in-One random prime labeling mixture (Sigma). Standard prehybridization, hybridization, and washing procedures were used (21).

Quantitative Real-time PCR

Real-time PCR conditions and oligonucleotides to measure mRNA levels for *Acly*, *Acs2*, acetyl-CoA carboxylase, fatty acid synthase, stearoyl-CoA desaturase 1, glycerol-3-phosphate-acyltransferase, long-chain fatty acyl elongase, glucose-6-phosphatase, glucokinase, glucose-6-phosphate dehydrogenase, malic enzyme, 3-hydroxy-3-methylglutaryl-CoA synthase, and 3-hydroxy-3-methylglutaryl-CoA reductase were described previously (22). The level of *Gapdh* mRNA was used as a control.

Western Blot Analysis

Fresh mouse tissues (liver, white adipose tissue, kidney, and brain) (0.5–1 g), or embryonic fibroblasts (grown to 80–90% confluency in 100-mm Petri dishes) were homogenized in RIPA buffer containing a mixture of protease inhibitors (Complete Mini EDTA-free, Roche Applied Science). Samples were incubated on ice for 30 min and centrifuged at 14,000 rpm for 10 min at 4 °C. The protein content of the supernatant fluid was determined with the Bradford assay (Bio-Rad). Denatured proteins (60–100 μg) were loaded onto precast 4–15% polyacrylamide gels (Bio-Rad). After electrotransfer onto polyvinylidene difluoride membrane (Amersham Biosciences), blots were blocked with phosphate-buffered saline containing 0.1% Tween and 3% bovine serum albumin for 4 h at 4 °C and incubated for 1 h at room temperature with a rabbit antibody against rat Acly (14) at a dilution of 1:500 in phosphate-buffered saline containing 0.10% bovine serum albumin. Blots were then incubated with a horseradish peroxidase-linked donkey anti-rabbit IgG antibody (Amersham Biosciences) at a dilution of 1:50,000 in phosphate-buffered saline containing 0.1% bovine serum albumin for 45 min at room temperature. Antibody binding was detected with the ECL Plus Western blotting kit (Amersham Biosciences); the blots were exposed to Hyperfilm ECL (Amersham Biosciences) and quantified by densitometry as described above.

Immunohistochemistry and β-Galactosidase Staining

Mice were anesthetized with avertin and perfusion-fixed with 4% paraformaldehyde. Tissues were harvested and fixed in 10% formalin for 4 h at 4 °C, immersed in 30% glucose for ~16 h at 4 °C, and frozen in O.C.T. (Sakura Finetek, Torrance, CA) for cryostat sectioning. β-Galactosidase activity was assessed by incubating 10-μm thick sections with a staining solution

containing 1.3 mg/ml 5-bromo-4-chloro-3-indolyl-β-D-galactopyranoside (X-gal) (Invitrogen) for 16 h at 37 °C (23). After staining, slides were counterstained with Eosin Y (Sigma). In some experiments, β-galactosidase staining was followed by immunohistochemistry. The following primary antibodies were used: rabbit anti-human glial fibrillary acidic protein (Sigma, 1:1,000), mouse monoclonal anti-neuronal nuclei (Chemicon, Temecula, CA, 1:1,000), goat anti-human choline acetyltransferase (Chemicon, 1:1,000), and goat anti-rat vesicular acetylcholine transporter (Chemicon, 1:5,000). Sections were subsequently incubated with the appropriate biotinylated secondary antibody (anti-rabbit or anti-goat IgG), and antigen-antibody complexes were detected after incubation with horseradish peroxidase and diaminobenzidine substrate (ABC kit, Vector Laboratories, Burlingame, CA). Sections were examined and photographed on an Eclipse 6600 microscope (Nikon, Japan) equipped with a Spot RT Slider digital camera (Diagnostic Instruments, Burlingame, CA).

RESULTS

The insertional mutation in the first intron of *Acly* introduced a new EcoRV site, making it possible to use Southern blots to distinguish between a 29.2-kilobase (kb) EcoRV fragment in the wild-type allele and a shorter (~6.2-kb) EcoRV fragment in the mutant allele (Fig. 1*A*). The mutation results in the production of a fusion transcript containing sequences from exon 1 joined to β*geo* (Fig. 1*B*). There is little doubt that the insertional mutation inactivated *Acly*. *Acly* mRNA levels were decreased by ~50% in *Acly*+/− mice (Fig. 1*B*), as were Acly protein levels (Fig. 1*C*).

Acly+/− mice were intercrossed in an attempt to obtain homozygous knockout mice. However, genotyping of more than 60 litters did not yield any homozygous mice. Moreover, we genotyped more than 80 embryos from 8.5 to 17.5 dpc, and found no homozygous knockout embryos. *Acly* is expressed at high levels throughout embryonic development (Fig. 2*A*), and β-galactosidase staining revealed that *Acly* is expressed at high levels in the neural tube at 8.5 dpc (Fig. 2*B*). We concluded that *Acly* expression in embryos is required for development.

We predicted that *Acly*+/− mice would have reduced body weight and lower plasma lipid levels as a consequence of a reduced capability for lipid synthesis. However, the levels of cholesterol, triglycerides, and free fatty acids in the plasma were no different in chow-fed *Acly*+/+ and *Acly* +/− mice (Table I). Moreover, feeding the mice a Western diet did not yield any significant difference in plasma lipid levels (Table I) or in hepatic cholesterol and triglyceride levels (not shown). Body weights of *Acly*+/+ and *Acly*+/− mice were virtually identical (Table I).

We suspected that *Acly*+/− mice might exhibit reduced weight gain and lower plasma lipid levels when fed a high-carbohydrate diet, which results in high levels of *de novo* lipogenesis in the liver. Contrary to our hypothesis, however, body weights and plasma levels of cholesterol, triglycerides, free fatty acids, and glucose were similar in *Acly*+/+ and *Acly*+/− mice over 3 months of observation (Table II). Also, feeding the carbohydrate-rich diet to *Acly* +/− mice was not associated with reduced liver stores of cholesterol and triglycerides (Table III).

We also examined lipid synthesis in primary fibroblasts from *Acly*+/+ and *Acly*+/− embryos. As expected, *Acly* mRNA (Fig. 3*A*) and protein levels (Fig. 3*B*) were reduced by ~50% in heterozygous cells. However, the amount of cholesterol synthesis in *Acly*+/+ and *Acly*+/− fibroblasts was similar, as judged by [^{14}C]citrate metabolic labeling experiments (Fig. 3*C*). It was not possible to assess the impact of reduced *Acly* expression on triglyceride synthesis, because very little [^{14}C]citrate was incorporated into triglycerides. However, *Acly*+/+ and *Acly* +/− fibroblasts displayed similar amounts of triglyceride synthesis in [^{3}H]glycerol labeling

experiments (Fig. 3*C*). Similarly, cholesterol and triglyceride synthesis rates were entirely normal in primary hepatocytes from *Acly*+/− mice (Fig. 4).

The fact that the *Acly*+/− mice and *Acly*+/− cells did not manifest detectable perturbations in lipid levels or lipid biosynthesis suggested that half-normal levels of Acly have little impact on cellular lipid homeostasis. Indeed, this appeared to be the case. As judged by quantitative reverse transcriptase-PCR, *Acly* mRNA levels were reduced by 50% in *Acly*+/− cells, but the expression of a host of other enzymes involved in triglyceride, cholesterol, and glucose metabolism was not perturbed (Figs. 3*D* and 5*A*). Of note, the half-normal levels of *Acly* expression did not lead to an up-regulation of the expression of *Asc1*, the other acetyl-CoA-synthesizing enzyme in the cytosol (Figs. 3*A* and 5*B*). In keeping with the latter finding, the synthesis of cholesterol and triglycerides from [^{14}C]acetate (a measure of Acs1 activity (2)) was identical in *Acly*+/+ and *Acly*+/− cells (Fig. 3*C*).

Northern blots showed that *Acly* is expressed in multiple tissues (Fig. 6*A*). To explore the cell-type specific expression patterns, sections of tissues from *Acly*+/− mice were stained for β-galactosidase expression. Strong β-galactosidase expression was identified in multiple cell types, including Leydig cells in testis (Fig. 6*B*) and renal tubular cells (Fig. 6*C*). In the livers of chow-fed mice, β-galactosidase staining was largely confined to the periportal hepatocytes (Fig. 6*D*). In mice fed a fat-free, carbohydrate-rich diet, β-galactosidase staining of the liver was much more widespread and more intense (Fig. 6*E*), reflecting increased levels of *Acly* expression (Fig. 6*G*). On the Western diet, β-galactosidase staining of the liver was only modestly increased, compared with the chow diet (Fig. 6*F*).

β-Galactosidase expression was intense throughout the brains of 15.5 dpc *Acly*+/− embryos (Fig. 7*A*) and 1-day-old *Acly*+/− pups (Fig. 7*B*), consistent with the presumed role of Acly in the *de novo* lipogenesis required for myelin formation (14). We suspected that *Acly* expression in the brain would decrease in older animals, mirroring a reduced requirement for lipid synthesis (24–28). This suspicion was confirmed. In 3-week-old pups, β-galactosidase staining was less intense than in the 1-day-old mice, although staining was still observed in the hippocampus, thalamus, medulla, and the white matter of cerebellum (Fig. 7*C*). In 6-month-old mice, *Acly* was expressed at far lower levels in the brain than in the younger mice (Fig. 7*D*). In the adult mice, β-galactosidase was expressed in glial cells (Fig. 8*A*) and in neurons (Fig. 8*B*).

Although the overall level of β-galactosidase expression was much lower in adult brains than in embryos, discrete regions of the adult brain showed very intense β-galactosidase staining. For example, relatively high levels of *Acly* expression persisted in hippocampus, the granular layer of the cerebellum, and other specific regions within the cerebellum, pons, medulla, and spinal cord (Fig. 7*D*). The facial nucleus in the medulla stained intensely for β-galactosidase (Fig. 7*D*), as did the gray matter of the spinal cord, particularly the ventral horns (Fig. 8*C*).

Initially, we hypothesized that the regions of the adult brain that stained highly for β-galactosidase were simply a subset of neurons with a high metabolic requirement for new lipid synthesis. Later, however, we remembered that acetyl-CoA is a key substrate for choline acetyltransferase in the synthesis of acetylcholine, and we became attracted to the hypothesis that those cells might be *cholinergic* neurons. To test this hypothesis, we stained histological sections for *Acly* expression (*i.e.* β-galactosidase) and two markers of cholinergic neurons, choline acetyltransferase and vesicular acetylcholine transporter. Indeed, *Acly* (Fig. 9*A*) and choline acetyltransferase (Fig. 9*B*) displayed strikingly overlapping patterns of expression in the hippocampus, as did *Acly* and vesicular acetylcholine transporter (Fig. 9*C*). *Acly* and vesicular acetylcholine transporter also colocalized in Purkinje cells of the cerebellum (Fig. 9*E*) and in several cerebellar nuclei (Fig. 9*F*). Finally, *Acly* was expressed very highly in

vesicular acetylcholine transporter-expressing neurons in the facial nucleus within the medulla (Fig. 9*H*).

DISCUSSION

In the current study, we created *Acly* knockout mice in which a β-galactosidase marker is expressed from *Acly* regulatory sequences, with the goal of further elucidating the physiologic roles of *Acly* in mammals. *Acly* is clearly required for embryonic development: no viable homozygous *Acly* knockout embryos were identified. The other enzyme capable of producing acetyl-CoA in the cytosol, Acs1, was evidently not sufficient to support development. Knockout mouse experiments frequently offer up surprises, but the lethal developmental defect in the *Acly* knockout homozygotes probably makes perfect sense, given the central role of Acly in energy metabolism. Acly is important for generating acetyl-CoA from glycolysis and, in particular, is required for obtaining acetyl-CoA from mitochondria. Acetyl-CoA can also be generated within mitochondria, either by pyruvate dehydrogenase or by the β-oxidation of fatty acids. To be used for lipid synthesis in the cytosol, however, acetyl-CoA must be exported from the mitochondria. To accomplish the transfer, mitochondrial acetyl-CoA condenses with oxaloacetate to form citrate, which is then transported to the cytosol, where it is used by Acly to create acetyl-CoA. Hence, the elimination of Acly effectively prevents the export of lipid building blocks from mitochondria.

The fact that lipid homeostasis appeared to be totally unaffected by half-normal levels of Acly was unexpected. One possibility is that Acly is synthesized in abundant quantities and that half-normal levels of the enzyme are simply not limiting for acetyl-CoA production. Another possibility is suggested by the intrinsic enzymatic properties of Acly. Acly activity in mammals and lower organisms is allosterically regulated by one of its cosubstrates, citrate (29). It is therefore likely that even evanescent increases in intracellular citrate levels would stimulate enzyme activity and increase the conversion of citrate into acetyl-CoA, thereby preventing measurable metabolic effects (*e.g.* reduced lipid synthesis or perturbed expression of SREBP-regulated genes).

The β-galactosidase marker in the mutant *Acly* allele provides novel information on the cell type-specific expression of *Acly*. For example, the high levels of *Acly* expression in the testis revealed by Northern blot (14) are largely explained by high levels of β-galactosidase activity in Leydig cells. One could argue that this pattern of expression is not surprising, given the role of Leydig cells in the synthesis of a steroid hormone. On the other hand, we would maintain that this pattern was not entirely predictable *a priori*. Two other lipid biosynthetic genes that we have studied, phosphatidylserine synthase 2 and 1-acyl-*sn*-glycerol-3-phosphate acyltransferase 4, are expressed highly in testis but mainly in Sertoli cells (23),[2] which likely have a role in the delivery of lipid nutrients to the germ cells.

The expression of β-galactosidase in *Acly*+/− mice faithfully mirrored *Acly* expression. In mice fed a high-carbohydrate diet, high levels of *Acly* expression were detected by Northern blot in the liver, and the hepatocytes of those livers manifested a high level of β-galactosidase activity. Interestingly, *Acly* was clearly expressed predominantly in a periportal distribution. This study, as far as we are aware, is the first to allow the direct visualization of different levels of *de novo* lipogenesis in distinct zones of the liver.

The up-regulation of hepatic *Acly* expression on a high-carbohydrate diet is controlled at the transcriptional level by SREBP-1 (3,11,12). (In transgenic mice expressing a truncated form of SREBP-1c, *Acly* was one of the most up-regulated of all of the SREBP-controlled genes

[2]A. P. Beigneux, unpublished observations.

(11).) We suggest that the β-galactosidase marker in the mutant *Acly* allele could be a useful tool for visualizing SREBP-1c gene regulation *in vivo* in response to changing metabolic conditions. As far as we are aware, the mutant *Acly* allele reported here is the only such "SREBP activity marker" currently available.

β-Galactosidase staining proved to be useful in understanding the role of *Acly* in the brain. First, β-galactosidase expression was high in the developing brain and was much lower in older mice. That temporal expression pattern undoubtedly reflects different rates of *de novo* lipogenesis at different stages of development (26–28). *Acly* was expressed in both glial cells and neurons. Second, in adult mice, we identified very high levels of β-galactosidase expression in cholinergic neurons, particularly in the brain stem and spinal cord. Whereas one might conceivably argue that this β-galactosidase expression reflects some peculiar requirement of cholinergic neurons for high levels of lipid synthesis, we think it is more likely that the very intense staining of cholinergic neurons reflects a role for *Acly* in acetylcholine synthesis. This conclusion is not farfetched: acetyl-CoA is a cosubstrate for choline acetyltransferase, which produces acetylcholine. Moreover, citrate and hydroxycitrate stimulate and inhibit, respectively, the *in vitro* synthesis of acetylcholine in rat caudate nuclei (30) and perfused rat phrenic nerve (31). Also, acetyl-CoA levels in cells have been reported to correlate directly with the rate of *in vitro* acetylcholine synthesis in rat caudate nuclei (32) and SN56 hybrid cholinergic cells (33).

It has been suggested that Asc1 could play a role in the regeneration of acetyl-CoA from acetate that is taken up after the breakdown of acetylcholine by acetylcholinesterase in nerve synapses (34). Based on published Northern blot experiments, the level of *Asc1* expression in the brain is low (2,35). However, if *Asc1* is truly important for acetate metabolism in cholinergic neurons, we would predict that *Asc1*, like *Acly*, might be expressed highly in the cholinergic neurons of the brain stem and spinal cord. Finally, although both *Acly* and *Asc1* expression are unequivocally regulated by SREBP-1c (2,11), we speculate that the genetic regulation of *Acly* and *Asc1* expression in cholinergic neurons might be more complex, taking into account the additional requirement of those cells for acetyl-CoA for acetylcholine synthesis.

In summary, our data show that Acly is critically important for embryonic development of the mouse, but there were no defects in lipid synthesis in the setting of half-normal levels of Acly. Our studies clearly support a major role for *Acly* in lipid synthesis, and suggest that *Acly* expression in the adult brain is important for the production of acetyl-CoA for acetylcholine synthesis.

Acknowledgments

We thank Dr. Nabil A. Elshourbagy (SmithKline Beecham, King of Prussia, PA) for the antibody against rat Acly; Dr. Lorenzo Arnaboldi for technical advice and lipid analyses; and S. Ordway and G. Howard for comments on the manuscript. We thank Dr. Jacquelyn J. Maher, Gene Lee, and Claudio Villanueva for help in preparing primary hepatocytes.

REFERENCES

1. Knowles SE, Jarrett IG, Filsell OH, Ballard FJ. Biochem. J 1974;142:401–411. [PubMed: 4441381]
2. Luong A, Hannah VC, Brown MS, Goldstein JL. J. Biol. Chem 2000;275:26458–26466. [PubMed: 10843999]
3. Liang G, Yang J, Horton JD, Hammer RE, Goldstein JL, Brown MS. J. Biol. Chem 2002;277:9520–9528. [PubMed: 11782483]
4. Sullivan AC, Triscari J, Hamilton JG, Miller ON, Wheatley VR. Lipids 1974;9:121–128. [PubMed: 4815799]
5. Bray GA, Greenway FL. Clin. Endocrinol. Metab 1976;5:455–479. [PubMed: 821680]

6. Chee H, Romsos DR, Leveille GA. J. Nutr 1977;107:112–119. [PubMed: 833671]
7. Greenwood MR, Cleary MP, Gruen R, Blase D, Stern JS, Triscari J, Sullivan AC. Am. J. Physiol 1981;240:E72–E78. [PubMed: 7457600]
8. Saxty BA, Novelli R, Dolle RE, Kruse LI, Reid DG, Camilleri P, Wells TN. Eur. J. Biochem 1991;202:889–896. [PubMed: 1765100]
9. Pearce NJ, Yates JW, Berkhout TA, Jackson B, Tew D, Boyd H, Camilleri P, Sweeney P, Gribble AD, Shaw A, Groot PH. Biochem. J 1998;334:113–119. [PubMed: 9693110]
10. Leonhardt M, Hrupka B, Langhans W. Physiol. Behav 2001;74:191–196. [PubMed: 11564468]
11. Shimomura I, Shimano H, Korn BS, Bashmakov Y, Horton JD. J. Biol. Chem 1998;273:35299–35306. [PubMed: 9857071]
12. Shimano H, Yahagi N, Amemiya-Kudo M, Hasty AH, Osuga J, Tamura Y, Shionoiri F, Iizuka Y, Ohashi K, Harada K, Gotoda T, Ishibashi S, Yamada N. J. Biol. Chem 1999;274:35832–35839. [PubMed: 10585467]
13. Dietschy JM, Turley SD. Curr. Opin. Lipidol 2001;12:105–112. [PubMed: 11264981]
14. Elshourbagy NA, Near JC, Kmetz PJ, Sathe GM, Southan C, Strickler JE, Gross M, Young JF, Wells TN, Groot PH. J. Biol. Chem 1990;265:1430–1435. [PubMed: 2295639]
15. Foster DW, Srere PA. J. Biol. Chem 1968;243:1926–1930. [PubMed: 5646484]
16. Melnick JZ, Srere PA, Elshourbagy NA, Moe OW, Preisig PA, Alpern RJ. J. Clin. Invest 1996;98:2381–2387. [PubMed: 8941657]
17. Stryke D, Kawamoto M, Huang CC, Johns SJ, King LA, Harper CA, Meng EC, Lee RE, Yee A, L'Italien L, Chuang PT, Young SG, Skarnes WC, Babbitt PC, Ferrin TE. Nucleic Acids Res 2003;31:278–281. [PubMed: 12520002]
18. Townley DJ, Avery BJ, Rosen B, Skarnes WC. Genome Res 1997;7:293–298. [PubMed: 9074932]
19. Björkegren J, Beigneux A, Bergo MO, Maher JJ, Young SG. J. Biol. Chem 2002;277:5476–5483. [PubMed: 11739387]
20. Shimano H, Horton JD, Hammer RE, Shimomura I, Brown MS, Goldstein JL. J. Clin. Invest 1996;98:1575–1584. [PubMed: 8833906]
21. Beigneux A, Withycombe SK, Digits JA, Tschantz WR, Weinbaum CA, Griffey SM, Bergo M, Casey PJ, Young SG. J. Biol. Chem 2002;277:38358–38363. [PubMed: 12151402]
22. Moon YA, Horton JD. J. Biol. Chem 2003;278:7335–7343. [PubMed: 12482854]
23. Bergo MO, Gavino BJ, Steenbergen R, Sturbois B, Parlow AF, Sanan DA, Skarnes WC, Vance JE, Young SG. J. Biol. Chem 2002;277:47701–47708. [PubMed: 12361952]
24. Spady DK, Dietschy JM. J. Lipid Res 1983;24:303–315. [PubMed: 6842086]
25. Dietschy JM, Kita T, Suckling KE, Goldstein JL, Brown MS. J. Lipid Res 1983;24:469–480. [PubMed: 6304219]
26. Jurevics H, Morell P. J. Neurochem 1995;64:895–901. [PubMed: 7830084]
27. Jurevics HA, Kidwai FZ, Morell P. J. Lipid Res 1997;38:723–733. [PubMed: 9144087]
28. Turley SD, Burns DK, Dietschy JM. Am. J. Physiol 1998;274:E1099–E1105. [PubMed: 9611162]
29. Barnum, TE. Enzyme Handbook. New York: Springer-Verlag; 1969.
30. Ricny J, Tucek S. J. Neurochem 1982;39:668–673. [PubMed: 6808088]
31. Endemann G, Brunengraber H. J. Biol. Chem 1980;255:11091–11093. [PubMed: 7440531]
32. Ricny J, Tucek S. Biochem. J 1980;188:683–688. [PubMed: 7470027]
33. Szutowicz A, Jankowska A, Blusztajn JK, Tomaszewicz M. J. Neurosci. Res 1999;57:131–136. [PubMed: 10397643]
34. Carroll PT. Brain Res 1997;753:47–55. [PubMed: 9125430]
35. Fujino T, Kondo J, Ishikawa M, Morikawa K, Yamamoto TT. J. Biol. Chem 2001;276:11420–11426. [PubMed: 11150295]

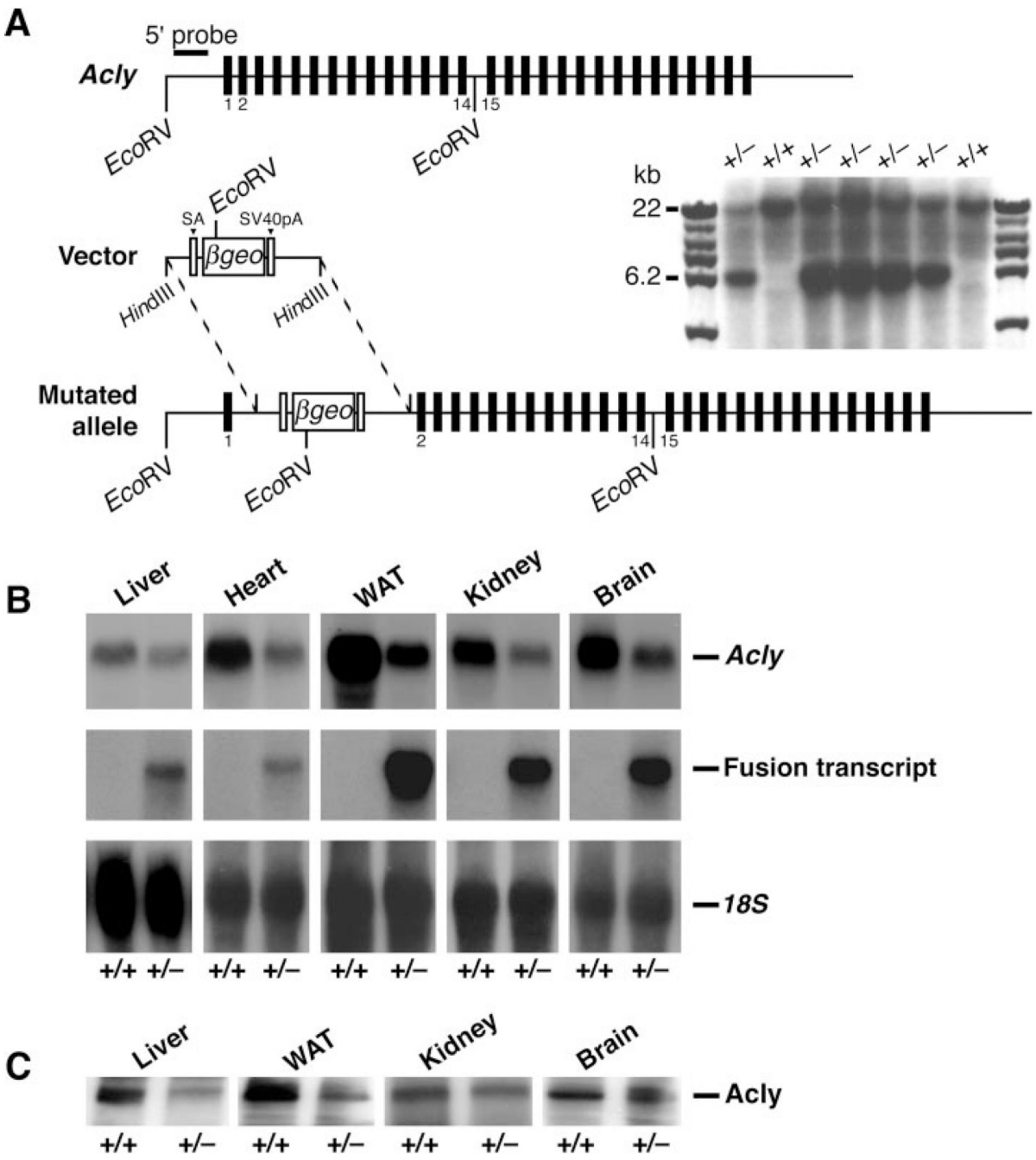

Fig. 1. Insertional mutation in *Acly*

A, schematic of the insertional mutation in *Acly*. Cell lines and mice were genotyped by Southern blot with a 5′ flanking probe. *Black boxes* represent exons. *SA*, splice acceptor; *SV40pA*, simian virus poly adenylation signal sequence. *B*, Northern blot of total RNA from liver, heart, white adipose tissue (*WAT*), kidney, and brain of *Acly*+/+ and *Acly*+/− mice. Three probes were used: an *Acly* cDNA, a β-galactosidase cDNA, and an *18S* cDNA (for normalization). *C*, Western blot of protein extracts from liver, WAT, kidney, and brain of *Acly* +/+ and *Acly*+/− mice with an Acly-specific antiserum.

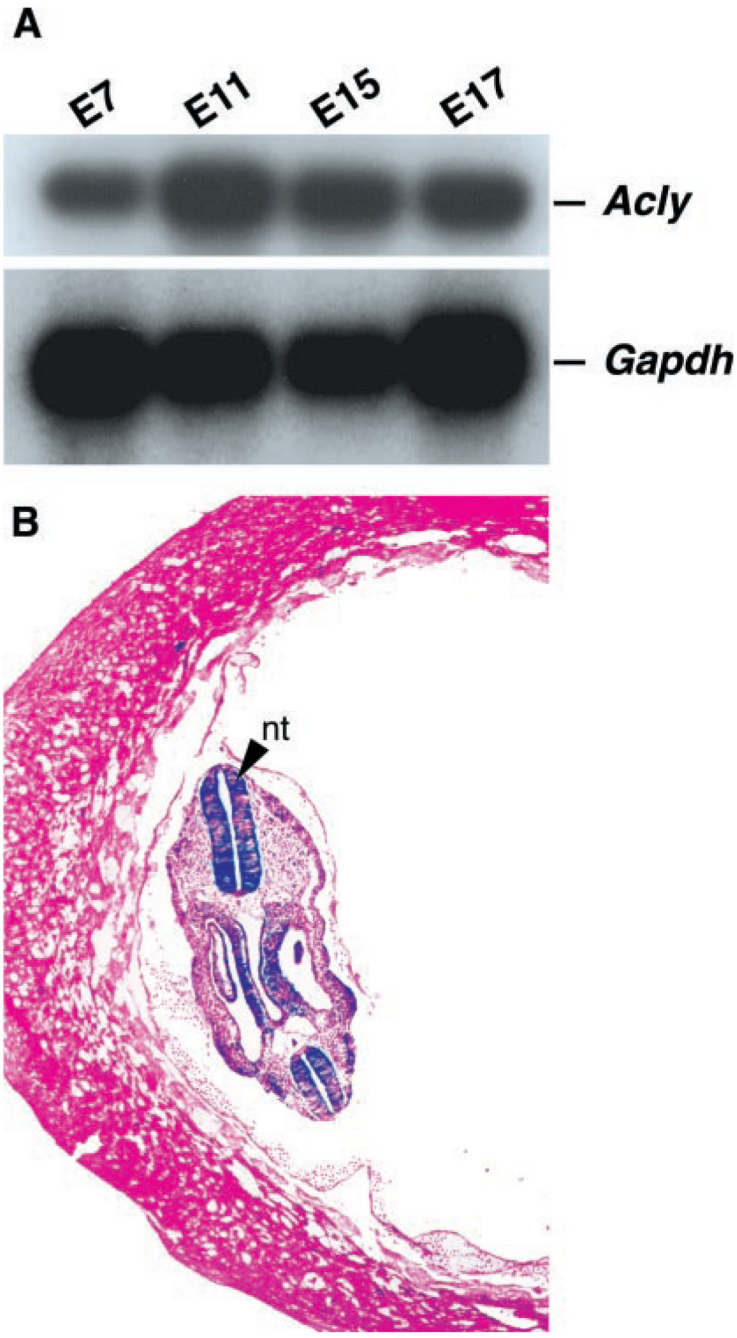

Fig. 2. Expression of *Acly* during development

A, mouse embryo poly(A)$^+$ RNA blot demonstrating that *Acly* is expressed throughout development. *B*, β-galactosidase staining of an 8.5-dpc *Acly*+/− embryo showing very high levels of *Acly* expression in the neural tube (*nt*). Original magnification, ×4.

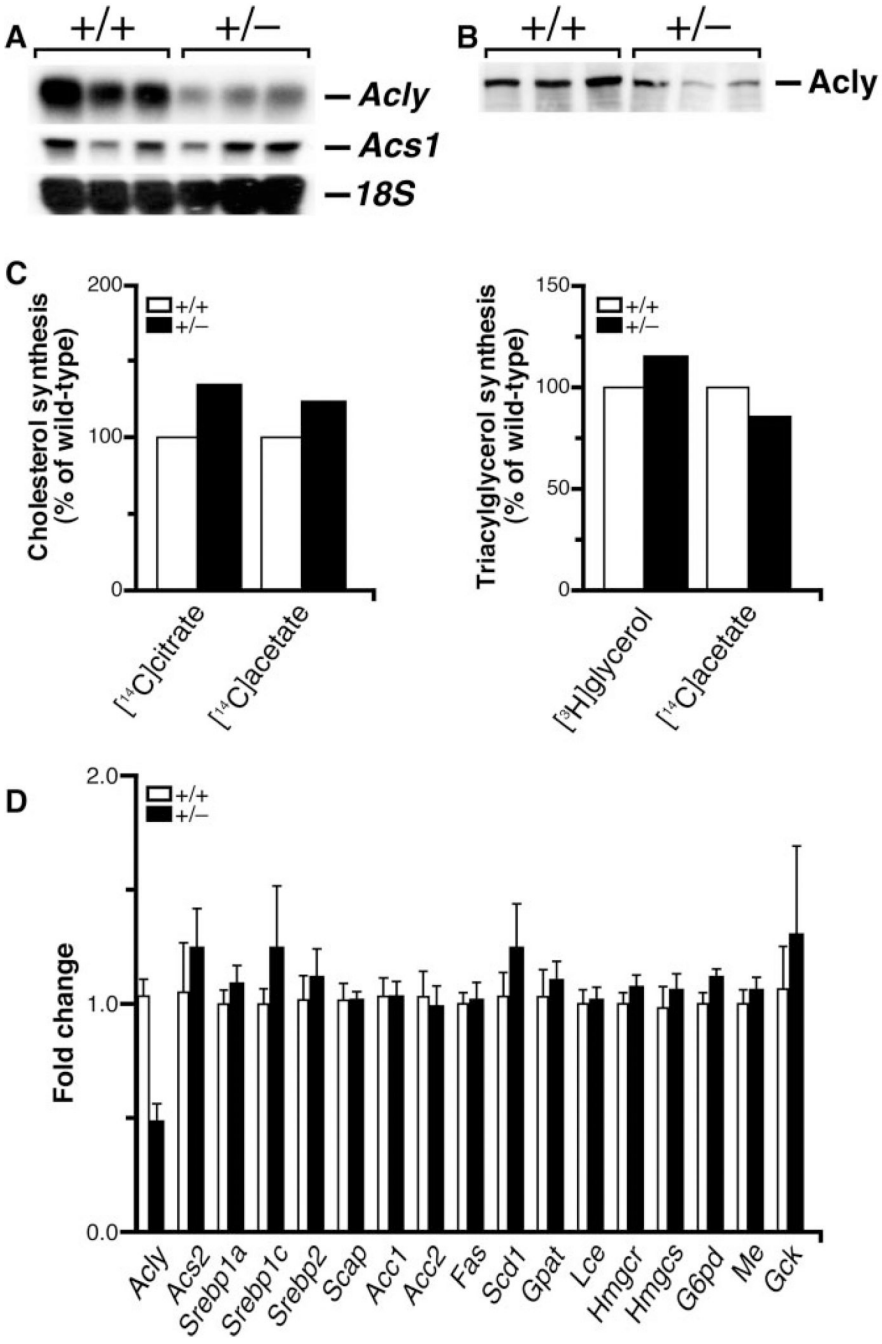

Fig. 3. Acly mRNA, protein, and activity levels in *Acly*+/+ and *Acly*+/− primary fibroblasts

A, Northern blot of total RNA from embryonic fibroblasts. Three probes were used: an *Acly* cDNA, an *Acs1* cDNA, and an *18S* cDNA (for normalization). *B*, Western blot of protein extracts from embryonic fibroblasts with an Acly-specific antiserum. *C*, cholesterol and triglyceride synthesis in embryonic fibroblasts. Cholesterol and triglyceride synthesis rates in *Acly*+/− cells are expressed as a percentage of those in *Acly*+/+ cells. The levels of incorporation into cholesterol in wild-type cells were: 2,289 cpm/mg of protein for [1,5-^{14}C]citric acid and 108,626 cpm/mg of protein for [1-^{14}C]acetic acid. The levels of incorporation into triglycerides in wild-type cells were: 34,560 cpm/mg of protein for [1(3)-^{3}H]glycerol and 26,882 cpm/mg of protein for [1-^{14}C]acetic acid. Data represent the average of duplicate determinations, and

each experiment was repeated twice. *D*, relative amount of mRNAs coding for a variety of enzymes involved in triglyceride, cholesterol, and glucose metabolism in *Acly*+/+ and *Acly*+/− embryonic fibroblasts. Total RNA was prepared from three cell lines per genotype. Equal aliquots were pooled according to genotype and analyzed by quantitative reverse transcription-PCR. *Gapdh* was used as a control in this experiment, although a cyclophilin control yielded virtually identical results. Values represent the relative amount of mRNA in relation to that measured in *Acly*+/+ fibroblasts. *Acc*, acetyl-CoA carboxylase; *Fas*, fatty acid synthase; *Scd1*, stearoyl-CoA desaturase 1; *Gpat*, glycerol-3-phosphate-acyltransferase; *Lce*, long-chain fatty acyl elongase; *G6pc*, glucose-6-phosphatase, catalytic; *Gck*, glucokinase; *G6pd*, glucose-6-phosphate dehydrogenase; *Me*, malic enzyme; *Hmgcs*, 3-hydroxy-3-methylglutaryl-CoA synthase; *Hmgcr*, 3-hydroxy-3-methylglutaryl-CoA reductase.

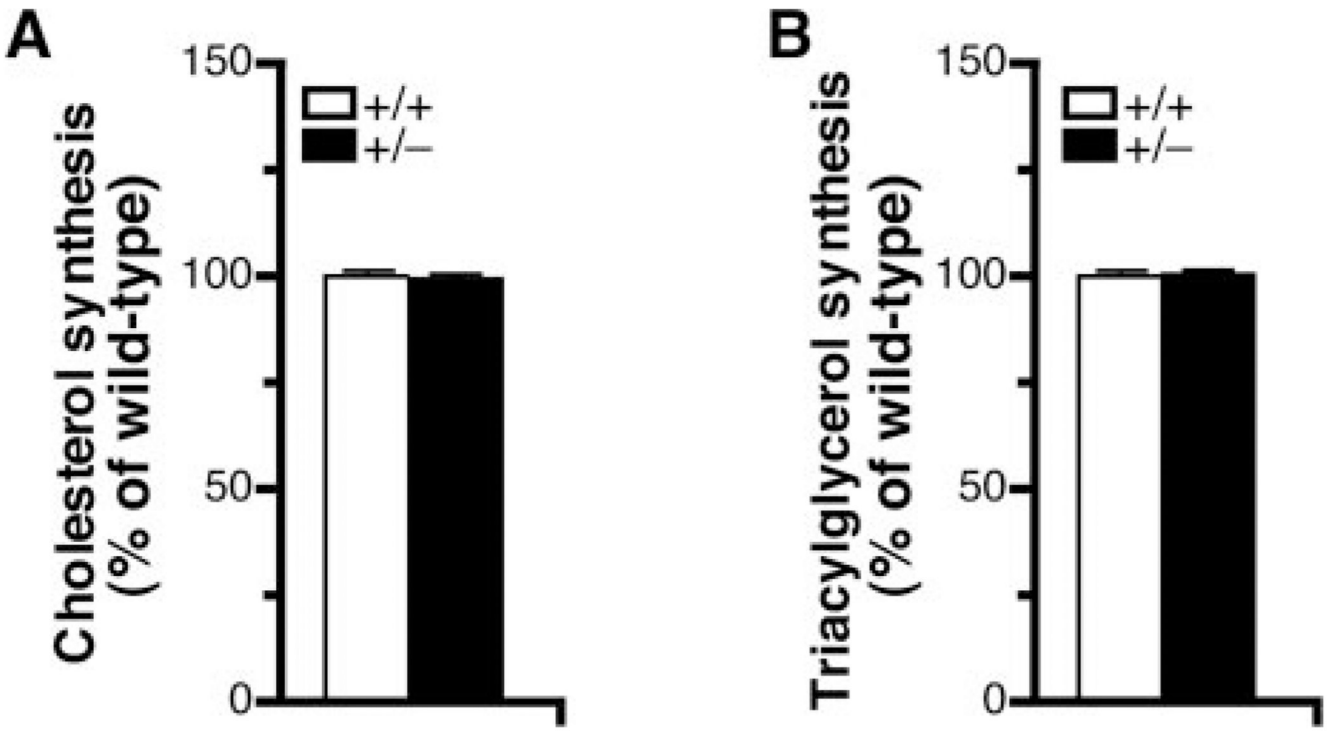

Fig. 4. Levels of cholesterol and triglyceride synthesis in primary hepatocytes from *Acly*+/+ and *Acly*+/− mice

Cholesterol and triglyceride synthesis rates in *Acly*+/− cells are expressed as a percentage of those in *Acly*+/+ cells. The levels of incorporation of [1(3)-^{3}H]glycerol into cholesterol and triglycerides in wild-type cells were 583 ± 33 cpm/μg of protein and 56,085 ± 2,919 cpm/μg of protein, respectively. Data represent the average of triplicate determinations, and each experiment was repeated twice.

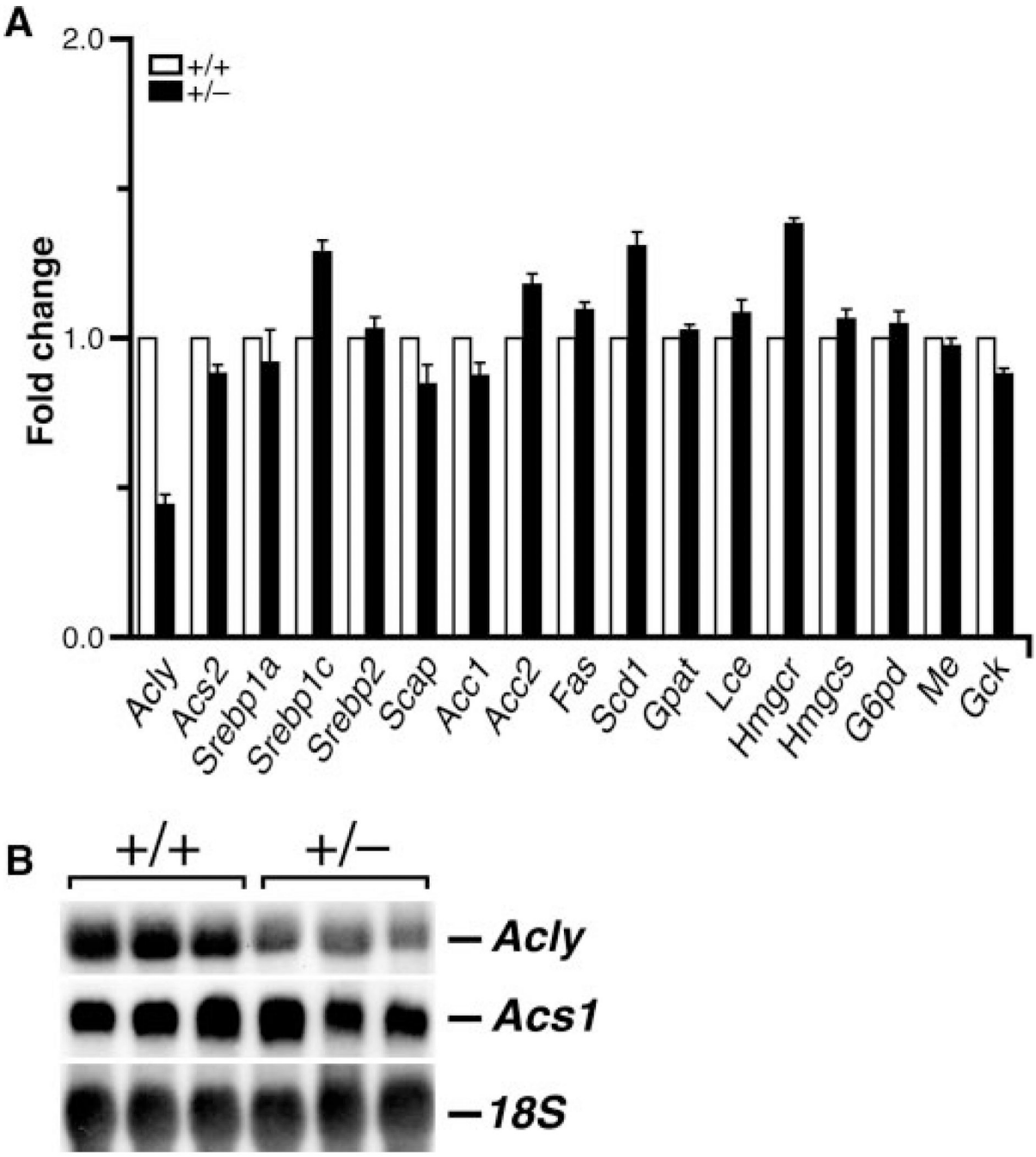

Fig. 5. Expression of *Acly*, *Acs1*, and lipid biosynthetic genes in liver from *Acly*+/+ and *Acly*+/− mice

A, relative amount of mRNAs coding for a variety of enzymes involved in triglyceride, cholesterol, and glucose metabolism in the livers of *Acly*+/+ and *Acly*+/− mice. Reverse transcriptase-PCR was performed as described in the legend to Fig. 3*D*. *B*, Northern blot of total RNA from liver. Three probes were used: *Acly* cDNA, *Acs1* cDNA, and *18S* cDNA (for normalization).

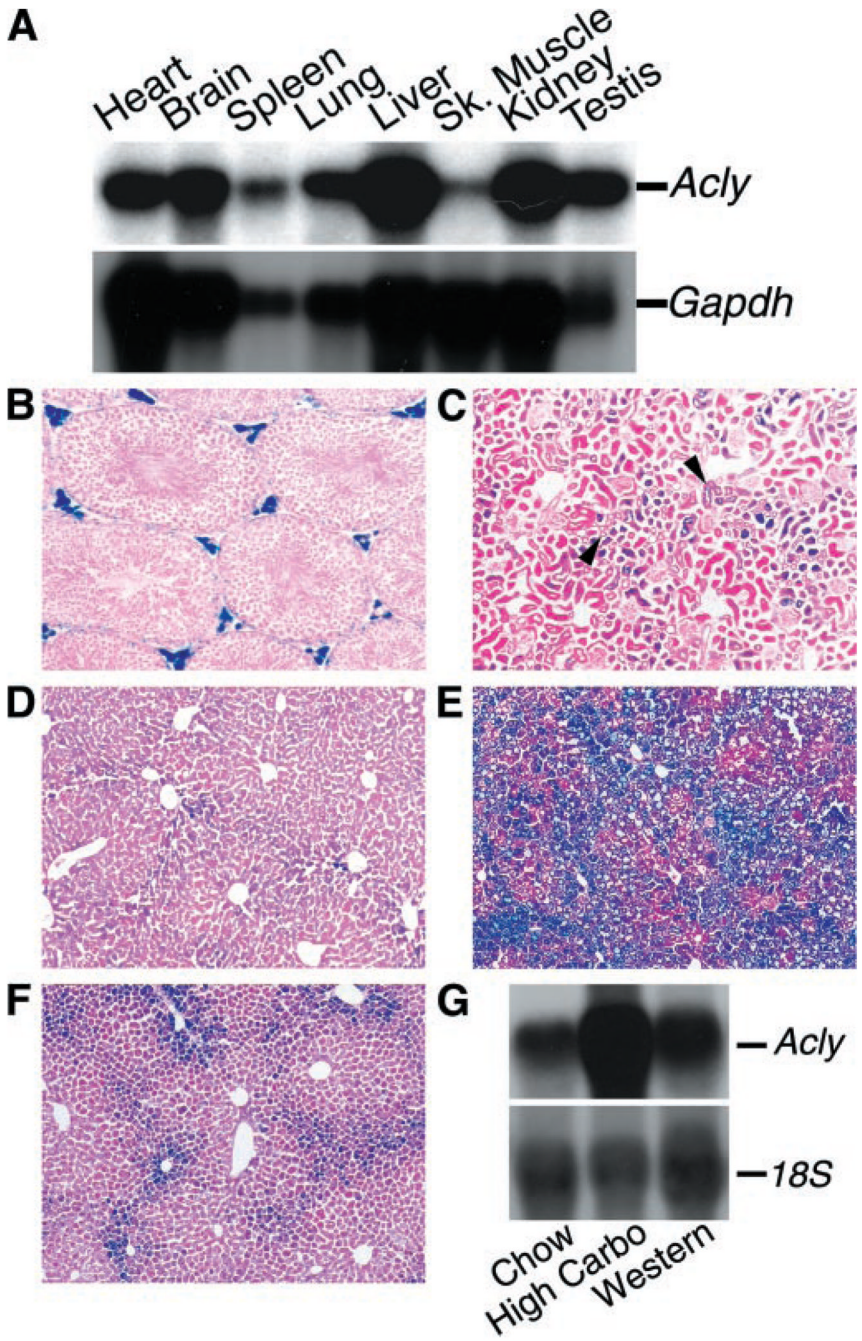

Fig. 6. Tissue pattern of *Acly* expression in adult mice and regulation of *Acly* expression in liver by diet

A, mouse multiple-tissue poly(A)$^+$ RNA blot showing *Acly* expression in the tissues of wild-type mice. A *Gapdh* cDNA was used for normalization. *B*, β-galactosidase staining of testis from a 4-week-old *Acly*+/− mouse, showing intense staining in Leydig cells. Original magnification, ×20. At higher power, less-intense staining of the Sertoli cells was also apparent. The same pattern of cellular expression was observed in testis from 7- and 36-week-old mice. *C*, β-galactosidase staining of a section of *Acly*+/− kidney. Original magnification, ×10. *Arrows* indicate tubules. *D–F*, β-galactosidase staining of liver from *Acly*+/− adult mice fed a chow diet (*D*), a fat-free, carbohydrate-rich diet (*E*), or a Western diet (*F*). Original

magnification, ×10. *G*, Northern blot analysis of total RNA from the liver of *Acly*+/+ mice on the three different diets. Two probes were used: *Acly* cDNA and *18S* cDNA (for normalization).

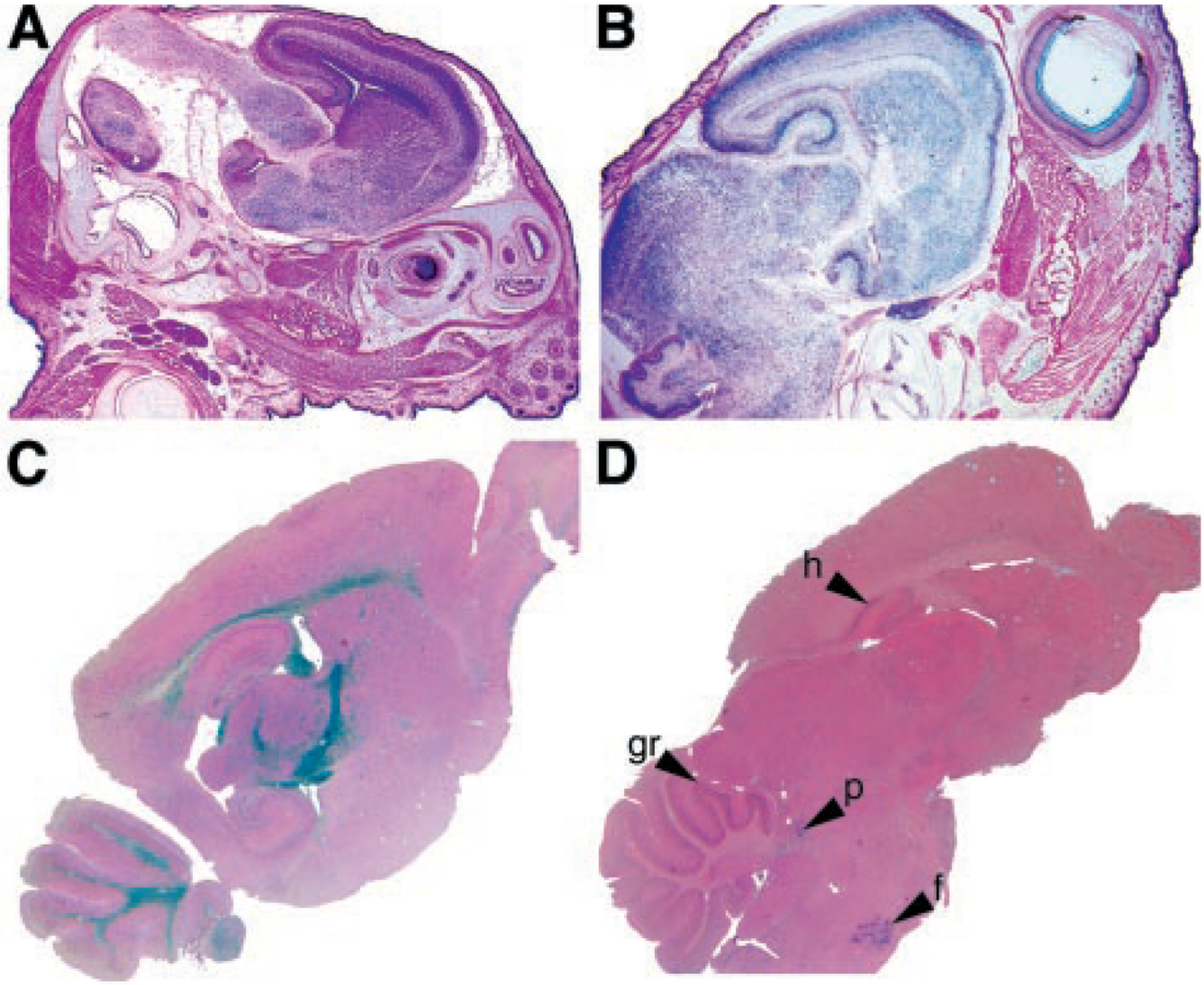

Fig. 7. Evolution of *Acly* expression in the maturing brain

A–D, β-galactosidase staining of sagittal sections of brains from a 15-dpc *Acly*+/− embryo (*A*), 1-day-old *Acly*+/− mouse (*B*), a 3-week-old *Acly*+/− mouse (*C*), and a 6-month-old *Acly* +/− mouse (*D*). Original magnifications, ×2 (*A* and *B*) and ×1 (*C* and *D*). *Arrows* indicate hippocampus (*h*), granular layer of the cerebellum (*gr*), nuclei of pons (*p*), and facial nucleus (*f*).

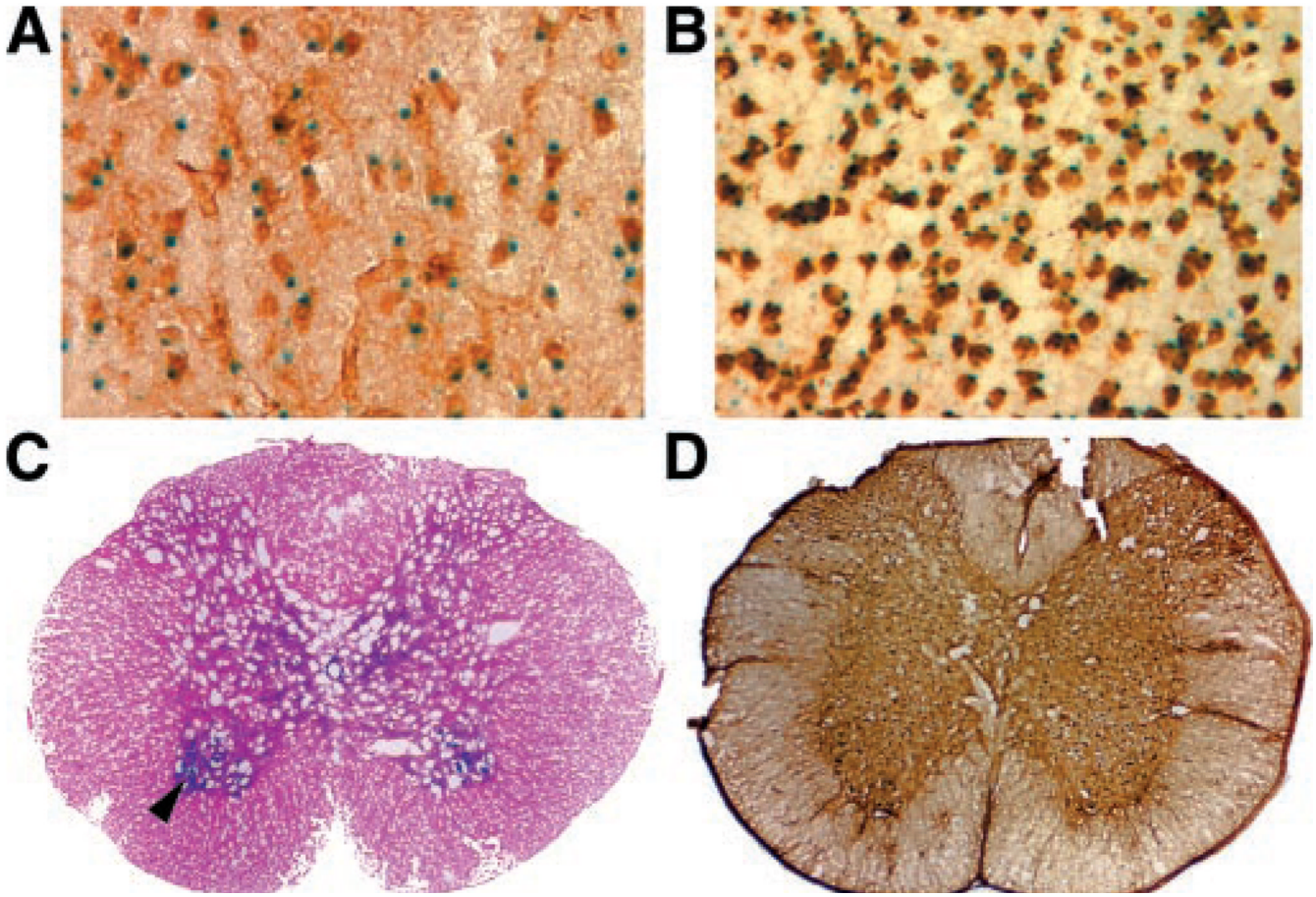

Fig. 8. *Acly* is expressed in glial cells and in neurons in the adult mouse nervous system

A and *B*, β-galactosidase and immunohistochemical staining of adult *Acly*+/− thalamus (*A*) and cortex (*B*). Specific antibodies against glial fibrillary acidic protein (*A*) and neuronal nuclei (*B*) were used. *C*, β-galactosidase staining of adult *Acly*+/− spinal cord (cervical). *Arrow* indicates ventral horn. *D*, immunohistochemical staining of adult *Acly*+/− spinal cord (cervical) with a specific antibody against neuronal nuclei. Original magnifications, ×40 (*A* and *B*) and ×4 (*C* and *D*).

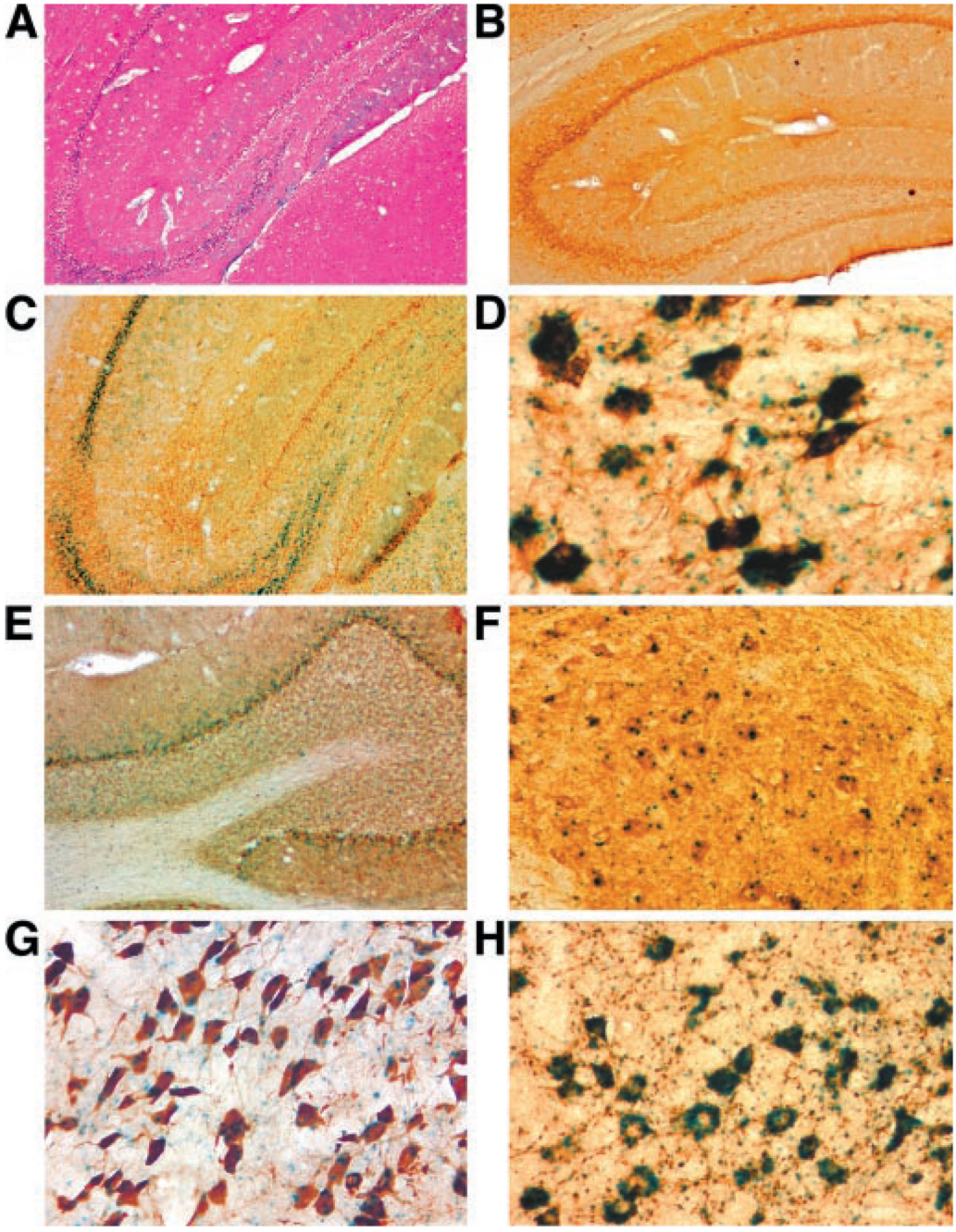

Fig. 9. *Acly* is expressed in cholinergic neurons in the adult mouse brain

A, β-galactosidase staining of a sagittal section of adult *Acly*+/− hippocampus. *B*, immunohistochemical staining of adult *Acly*+/− hippocampus with a specific antibody against choline acetyltransferase. *C–H*, β-galactosidase and immunohistochemical staining of adult *Acly*+/− hippocampus (*C*), pons nuclei (*D*), cerebellum (*E*), cerebellar nuclei (*F*), and medulla (facial nucleus) (*G* and *H*). Specific antibodies against vesicular acetylcholine transporter (*C*, *E*, and *H*), choline acetyltransferase (*F*), or neuronal nuclei (*D* and *G*) were used. Original magnifications, ×10 (*A–C* and *E*), ×20 (*F*), and ×40 (*D*, *G*, and *H*).

Table I

Plasma levels of cholesterol, triglycerides, and free fatty acids (FFA) in Acly+/+ and Acly+/− mice fed a Western diet

Mice were 3 weeks old at baseline.

	Baseline		1 month	
	+/+ (*n* = 18)	**+/− (*n* = 14)**	**+/+ (*n* = 18)**	**+/− (*n* = 14)**
Body weight (g)	20.6 ± 0.63	19.1 ± 1.07	33.0 ± 0.70	31.1 ± 1.13
Cholesterol (mg/dl)	83.4 ± 3.41	82.1 ± 3.61	148 ± 9.28	137 ± 8.34
Triglycerides (mg/dl)	67.4 ± 18.4	52.4 ± 14.6	129 ± 18.7	113 ± 14.2
FFA (μM)	411 ± 33.7	428 ± 70.6	688 ± 78.7	668 ± 106

Table II

Plasma levels of cholesterol, triglycerides, and free fatty acids (FFA) in Acly+/+ and Acly+/− mice fed a fat-free, carbohydrate-rich diet

Mice were 3 weeks old at baseline.

	Baseline		1 month	
	+/+ (*n* = 8)	**+/− (*n* = 8)**	**+/+ (*n* = 8)**	**+/− (*n* = 8)**
Body weight (g)	21.2 ± 0.80	18.5 ± 1.26	29.2 ± 1.24	26.4 ± 1.31
Cholesterol (mg/dl)	95.3 ± 5.00	85.3 ± 3.88	83.3 ± 16.4	78.8 ± 3.78
Triglycerides (mg/dl)	49.8 ± 8.25	42.6 ± 6.21	12.8 ± 2.37	14.1 ± 2.55
FFA (μM)	435 ± 50.1	428 ± 70.7	413 ± 61.4	318 ± 39.7

Table III

Hepatic cholesterol and triglyceride contents in Acly+/+ and Acly+/− mice fed a fat-free, carbohydrate-rich diet

Mice were 3 weeks old at baseline.

	Baseline		3 months	
	+/+ (*n* = 6)	**+/− (*n* = 14)**	**+/+ (*n* = 6)**	**+/− (*n* = 14)**
Cholesterol (mg/g protein)	7.88 ± 1.16	5.97 ± 0.77	32.3 ± 17.0	49.1 ± 7.21
Triglycerides (mg/g protein)	395 ± 39.0	361 ± 19.1	702 ± 207	628 ± 53.2